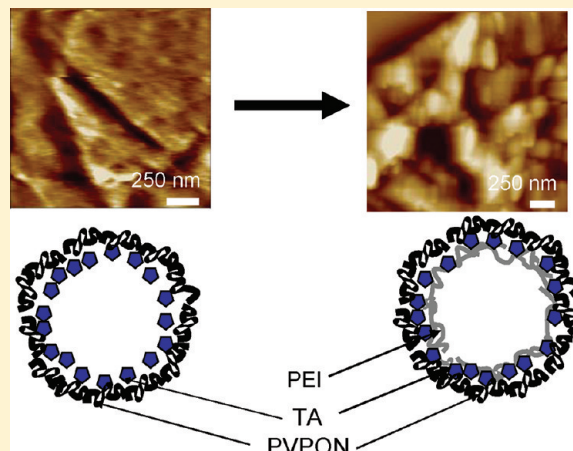


Direct Probing of Micromechanical Properties of Hydrogen-Bonded Layer-by-Layer Microcapsule Shells with Different Chemical Compositions

Milana O. Lisunova, Irina Drachuk, Olga A. Shchepelina, Kyle D. Anderson, and Vladimir V. Tsukruk*

School of Material Science and Engineering, Georgia Institute of Technology, Atlanta, Georgia 30332, United States

ABSTRACT: The mechanical properties of hydrogen-bonded layer-by-layer (LbL) microcapsule shells constructed from tannic acid (TA) and poly(vinylpyrrolidone) (PVPON) components have been studied in both the dry and swollen states. In the dry state, the value of the elastic modulus was measured to be within 0.6–0.7 GPa, which is lower than the typical elastic modulus for electrostatically assembled LbL shells. Threefold swelling of the LbL shells in water results in a significant reduction of the elastic modulus to values well below 1 MPa, which is typical value seen for highly compliant gel materials. The increase of the molecular weight of the PVPON component from 55 to 1300 kDa promotes chain entanglements and causes a stiffening of the LbL shells with a more than 2-fold increase in elastic modulus value. Moreover, adding a polyethylenimine prime layer to the LbL shell affects the growth of hydrogen-bonded multilayers which consequently results in dramatically stiffer, thicker, and rougher LbL shells with the elastic modulus increasing by more than an order of magnitude, up to 4.3 MPa. An alternation of the elastic properties of very compliant hydrogen-bonded shells by variation of molecular weight is a characteristic feature of weakly bonded LbL shells. Such an ability to alter the elastic modulus in a wide range is critically important for the design of highly compliant microcapsules with tunable mechanical stability, loading ability, and permeability.



INTRODUCTION

Layer-by-layer (LbL) microcapsules with different components show the ability for the incorporation and controlled release of a drug at a preselected set of conditions and for encapsulation of biological and chemical objects.^{1–9} One particular type, hydrogen-bonded LbL assemblies containing water-soluble polymers and weak polyacids, has received growing attention due to its high compliance, easy tunability, and responsiveness to environmental stimuli.^{10–13} The manipulation of these LbL films properties by changes in temperature or ionic strength makes hydrogen-bonded LbL films attractive candidates for controlled release applications.¹⁴ For instance, hydrogen-based LbL assembly is highly pH sensitive and could be completely disintegrated at higher pH values while surviving well at lower ones.^{11,12,15} Microcapsules with ultrathin hydrogen-bonded LbL shells have recently shown much promise for biomedical applications as they have been demonstrated to exhibit resistance toward cell adhesion and show a significant reduction in cytotoxicity.^{13,16–18} Hydrogen-bonded multilayers have also been utilized as antibacterial agents after films having been used as a matrix for the in-situ synthesis of silver nanoparticles.¹⁹

Tannic acid (TA) and poly(*N*-vinylpyrrolidone) (PVPON) have been widely exploited as versatile components for

hydrogen-bonded multilayer LbL films due to their ability to form stable complexes.^{20–22} Moreover, the TA/PVPON LbL assemblies have been established as stable shells for cell surface engineering with low cytotoxicity.^{16,23} High encapsulated cell viability, up to 94%, was achieved as opposed to about 20% viability in conventional poly(styrenesulfonate) (PSS)/poly(allylamine) (PAH) systems. It has been observed that the viability results depended critically upon the utilization of a polyethylenimine (PEI) prime layer during LbL assembly. However, fundamental reasons for this difference have not been established. The changes in shell permeability and possible softening/stiffening of LbL shells were suggested but not proven as playing a critical role.

Indeed, as well-known, the mechanical properties and strength of LbL shells define the deformational behavior and rupture mechanisms which are critical for cell surface engineering and loading/unloading behavior of the LbL microcapsules.^{24,25} This behavior can be tuned by different means including changes in the chemical composition and external conditions. As has been shown, softening of the ionic interactions between the

Received: June 3, 2011

Revised: July 23, 2011

Published: July 29, 2011

polyelectrolytes due to salt addition significantly affects mobility of the polyelectrolyte chains and shells permeability.^{26–29} The design of programmable microcapsules upon exposure to the mechanical triggering conditions was investigated by Esser-Kahn et al.³⁰ The effect of buckling transition on nonuniform layer distribution that leads to a reduction of wall thickness and thereby to an increase in the permeability was demonstrated by Gao et al.³¹ The strength of the intermolecular interactions could be significantly altered by chemical and physical cross-linking, encapsulation of the polymer prelayer, and also upon metal ion binding.^{32,33} For instance, the reduction of the elastic modulus of swollen PAH/PSS capsules has been demonstrated.³⁴ Zhang et al. have recently showed that the loading of Ag^+ to hydrogen-bonded multilayers of PVPON/poly(acrylic acid) (PAA) significantly improved the films stability even in acidic solution.¹⁸ In another approach, stabilization of hydrogen-bonded multilayer complexes through covalently, thermal, and photo-cross-linking has been demonstrated.^{2,35}

The mechanical properties of LbL films and shells are extensively studied by employing a battery of testing approaches. Among the most popular techniques is the buckling method applicable to planar films transferrable to an elastomeric substrate.^{36–39} Bulging testing with one-sided application of overpressure is widely used for the study of freely suspended LbL films.^{40–47} Methods of elastic properties evaluation employed to LbL shells are mainly based on osmotic/mechanical pressure and colloidal and surface force spectroscopy (CFS and SFS) techniques.^{24,48} The osmotic pressure method involves the observation of osmotically induced mechanical buckling of capsules immersed in a polyelectrolyte solution.^{31,49} The method requires an assumption on the rate of permeability of polyelectrolyte membrane that consequently might result in uncertainties of Young's modulus values obtained.⁵⁰ Also, the plastic deformation induced cannot be easily separated from the elastic deformation. The other method for elastic properties evaluation used a combination of reflection interference microscopy and CFS to evaluate the response of capsules made by LbL polyelectrolyte deposition.^{51–56} The method is limited by the assumption of full volume conservation and leads to the underestimation of the Young's modulus of a permeable membrane.

Finally, the SFS method is able to probe the local elastic properties and adhesive forces of a variety of polymer films and structures with nanoscale lateral and vertical resolution.^{60,57–60,61} SFS has been applied to LbL shells⁶² as well as for very thin LbL layers on solid substrates.^{63,64} Such a method does not depend upon geometrical properties of capsules, such as radius and wall thickness, and is independent of the permeability of the shell. SFS also allows application of very low forces to exclude plastic deformation and conduct measurements in a wide variety of environments, such as air and fluid and with AFM tips with modified chemical functionalities.^{65,66}

Overall, the measured modulus values for various LbL films ranged from extremely compliant around 1 MPa to relatively stiff with about 1 GPa in the swollen state and from 0.5 to 10 GPa in the dried, solid state.^{2,12,67–69,71,71} Such a wide variation in the elastic properties is caused by a difference in the nature of the components, a difference in intermolecular interactions, chain flexibilities, and preparation conditions such as pH conditions or changing the solvent component for core release. Overall, the mechanical properties of LbL microcapsules have been found to be in the same range as planar LbL films.⁷² However, possible additional effects resulting from the specific conditions of the

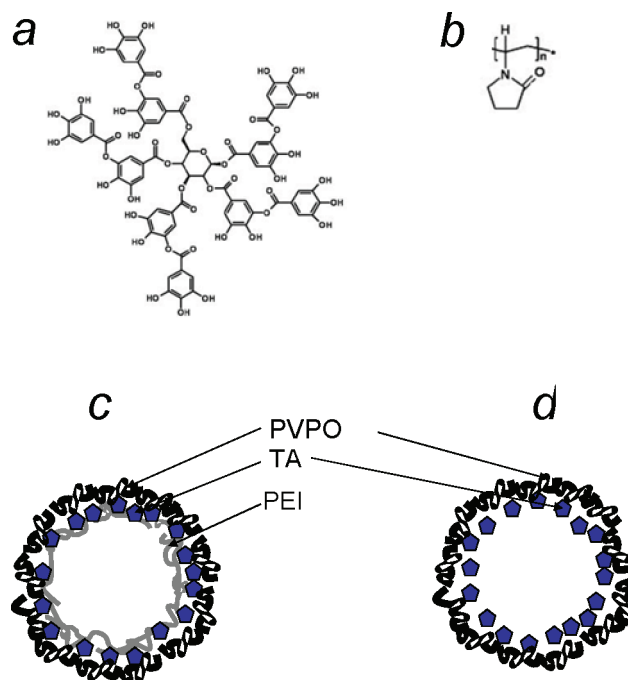


Figure 1. Chemical structures of TA (a) and PVPON (b) used in the hydrogen-bonded LbL assembly with (c) and without (d) PEI prime layer.

multilayer deposition on curved surfaces and core release procedure have not usually been considered.

In this study, the mechanical properties of hydrogen-bonded TA/PVPON LbL shells assembled on silica microparticles with and without PEI prime layer are probed in both dry and swollen states (Figure 1). We observed that, in the dry state, the value of the elastic modulus is within 0.6–0.7 GPa, but swelling of the LbL shells results in a dramatic reduction of the elastic modulus to around 0.2 MPa, which is a common value for highly compliant gel materials. This value is lower than that for traditional LbL shells made from polyelectrolytes and previously studied hydrogen-bonded LbL films. In contrast to polyelectrolyte-based LbL shells, the increase of the molecular weight of PVPON component as well as the addition of a PEI prime layer both promote significant stiffening of LbL shells with the elastic modulus rising by more than an order of magnitude.

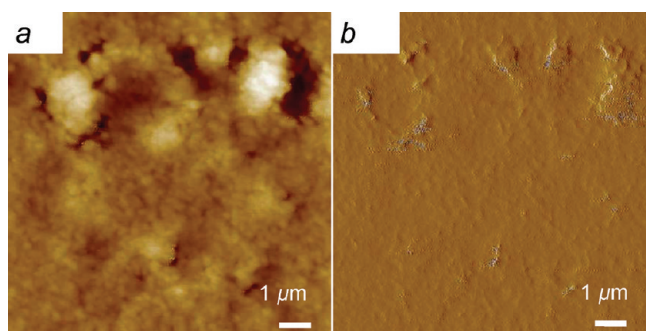
EXPERIMENTAL SECTION

Tannic acid (molecular weight (MW) = 1700 Da), PVPON of three molecular weights (55 000, 360 000, and 1 300 000 Da), branched polyethylenimine (25 000 Da), and mono- and dibasic sodium phosphate were purchased from Sigma-Aldrich. Silica particles with diameter $4.0 \pm 0.2 \mu\text{m}$ as 10% dispersions in water were obtained from Polysciences, Inc. Hydrofluoric acid (48–51%) was purchased from Aristar. Ultrapure water (Nanopure system) with a resistivity of 18.2 $\text{M}\Omega \text{ cm}$ was used in all experiments. Single-side polished silicon wafers of the {100} orientation (Semiconductor Processing Co.) were cut to a typical size of 10 mm \times 20 mm and cleaned in a piranha solution as described elsewhere.^{65,73}

The LbL deposition of $(\text{TA/PVPON})_4$ multilayers has been performed according to the established procedure.³² Briefly, 0.5 mg mL^{-1} polymer solutions were prepared by dissolving polymers in 0.01 M sodium phosphate buffer with pH adjusted to 5, except for PEI, which was dissolved in 0.1 M NaCl with pH adjusted to 7. Typical deposition

Table 1. Thickness, Microroughness, and Young's Modulus of Different Types of LbL Shells (All Shells Contain Four Bilayers) and Film, Respectively

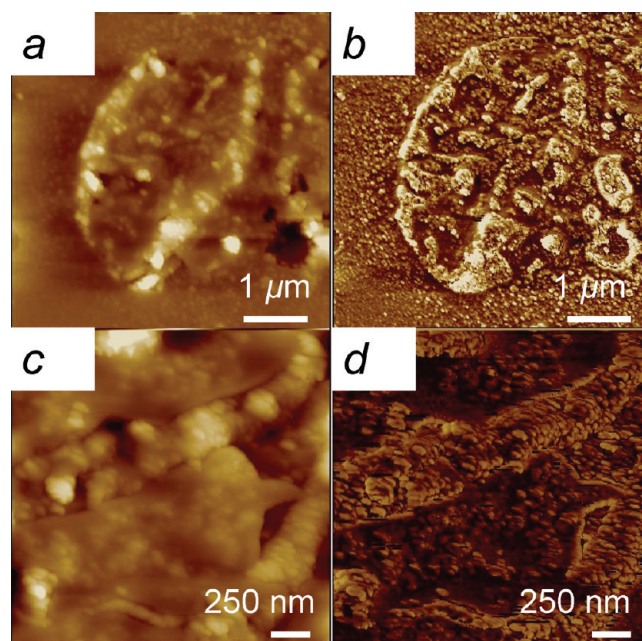
	thickness, nm		microroughness, nm		Young's modulus, MPa	
	dry	swollen	dry	swollen	dry	swollen
(TA/PVPON-360) ₄₀ film	55 ± 2		1.8 ± 0.5		700 ± 200	
TA/PVPON-55 shell	7.5 ± 1.2	12 ± 1.2	2.9 ± 0.3	3.3 ± 0.7		0.2 ± 0.03
TA/PVPON-360 shell	8.48 ± 3.4	12 ± 1.2	3.1 ± 1.0	4.5 ± 1.0		0.4 ± 0.02
TA/PVPON-1300 shell	13.5 ± 2.7	24.0 ± 2.4	3.4 ± 0.3	6.1 ± 2.5		0.45 ± 0.15
PEI(TA/PVPON-55) shell	7.5 ± 1.0	12.5 ± 1.3	3.3 ± 1.3	4.9 ± 0.9		0.89 ± 0.12
PEI(TA/PVPON-360) shell	13 ± 1.1	30 ± 3	3.4 ± 0.3	13.3 ± 2.0	600 ± 100	1.6 ± 0.2
PEI(TA/PVPON-1300) shell	15 ± 1.5	35.0 ± 1.2	3.9 ± 0.8	14.8 ± 2.3		4.3 ± 0.4

**Figure 2.** AFM topography (a) and phase (b) images of spin-deposited TA/PVPON-360 thin film. Z-scale is 20 nm (a) for topography image.

time was 15 min followed by three rinsing steps in phosphate buffer solution (0.01 M, pH = 5) to remove excess of polymer. For PEI-containing LbL microcapsules formation, a prelayer of branched-PEI was adsorbed first followed by alternate adsorption of (TA/PVPON) multilayer starting with TA. For particle suspensions, after each deposition step they were settled down by centrifugation at 2000 rpm for 2 min to remove the excess of polymer. Deposition, rinsing, and resuspending steps were performed on a VWR analogue vortex mixer at 2000 rpm. To etch out silica cores, the microparticles with the deposited multilayers were exposed to 8% hydrofluoric acid solution (HF) overnight followed by dialysis in ultrapure water for 36 h with repeated change of water. Direct deposition of (PVPON/TA)₄₀ multilayers on silicon substrates was performed at pH = 2 starting from a PVPON by dipping a substrate into an appropriate solution followed by three rinsing steps in 0.01 M phosphate buffer (pH = 5).

Topographical and phase images of the surface morphology of swollen and dried were observed under ambient conditions in the tapping and phase modes in fluid and in air, respectively, using a Dimension 3000 AFM microscope according to established procedures.^{66,74–76} The force–volume (FV) mode which utilizes the collection of the force–distance curves over selected surface areas was used for calculation histograms of elastic modulus and reduced adhesive forces. For micromapping we used 16 × 16 array with 1 μm × 1 μm selected surface area. Data collected were processed using a micromechanical analysis (MMA) software package.⁷⁷ AFM tip shape was determined by scanning a reference sample with gold nanoparticles. Values of microcantilever spring constants (within 0.04–10 N/m) used for force estimation have been obtained from thermal tuning. A special cantilever holder has been utilized for in-liquid measurements.

The static contact angle of ultrapure water on TA/PVPON-360 planar film was measured on a CAM 101 (KSV Instruments). Water droplets (5 μL) were placed randomly over the surface studied for static-contact-

**Figure 3.** AFM topography (a, c) and phase (b, d) images of TA/PVPON-1300 shell with PEI precursor in dried state. Z-scale is 180 nm (a) and 80 nm (c) for topography images.

angle measurements. The film thickness was determined using a M-2000U spectroscopic ellipsometer (Woollam) as described elsewhere.⁷⁸ Prior to the measurements, samples were dried with a stream of nitrogen.

RESULTS AND DISCUSSION

The results of AFM and SFS measurements of LbL films and shells are summarized in Table 1.

Planar LbL Films. Initially, we characterized the surface morphology and mechanical properties of (TA/PVPON-360)₄₀ film deposited on planar silicon wafers to elucidate benchmark values for further measurements for representative example. As we observed, these planar LbL films are relatively smooth with characteristic grainy morphology and few defects observed over microscopic surface areas (Figure 2). The microroughness is 1.8 ± 0.5 nm as measured within 300 nm × 300 nm surface areas (here and everywhere) which is common for hydrogen-bonded LbL films.³² The phase image is very homogeneous, confirming uniform surface composition of the film without noticeable segregation of components.

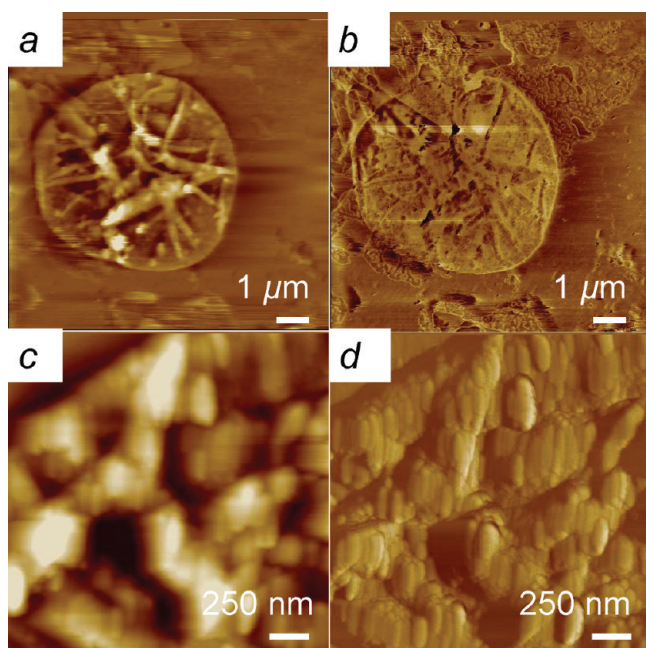


Figure 4. AFM topography (a, c) and phase (b, d) images of swollen TA/PVPON-1300 shell with PEI precursor in water. Z-scale is 450 nm (a) and 120 nm (c) for topography images. Elongated domain shapes are caused by creeping of LbL shells during scanning.

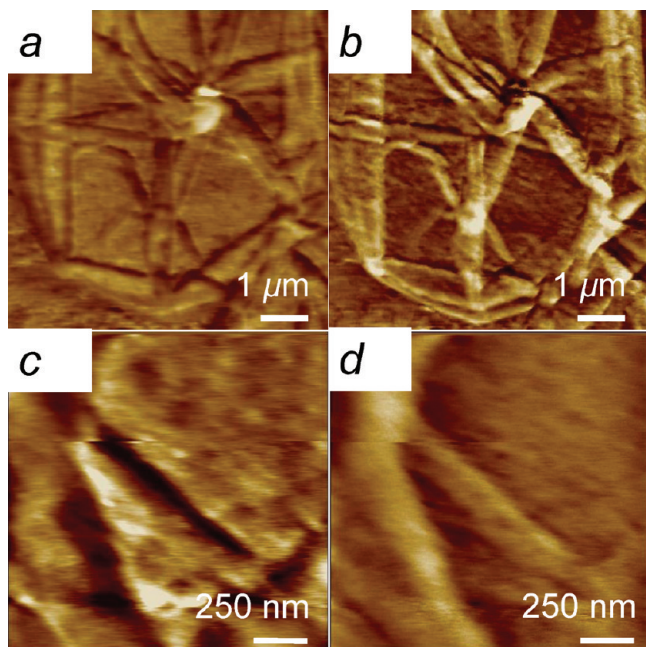


Figure 5. AFM topography (a, c) and phase (b, d) images of swollen TA/PVPON-1300 shell without PEI precursor in water. Z-scale is 200 nm (a) and 80 nm (c) for topography images.

The elastic modulus determined from loading curves in Sneddon's approximation (for detail see below) was determined to be 0.7 ± 0.2 GPa. The value of elastic modulus measured here is much lower than typical values of 2–6 GPa reported for polyelectrolyte-based LbL films.^{12,36} Such a significant lowering of the elastic modulus can be related to the overall weak

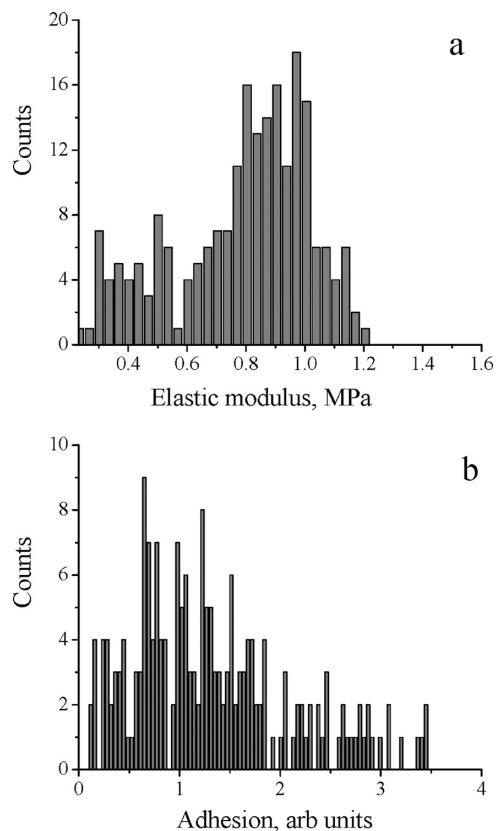


Figure 6. Histograms of the surface distribution of the elastic modulus (a) and adhesive force (b) of swollen PEI(TA/PVPON-55) shell in water. The histograms were derived from the force volume topography distribution by avoiding incorrect data from the damaged surface region. Histograms are taken from 16×16 arrays of force distance curves collected at $1 \mu\text{m} \times 1 \mu\text{m}$ surface area.

interactions and absence of dense ion pairing as well as residual water content. The plastification effect plays an even more important role in hydrogen-bonded LbL films than that in polyelectrolyte films.³⁶

Morphology of LbL Shells. The overall shape and fine morphology of collapsed LbL microcapsules have been observed with AFM imaging at different scales in the dried and swollen states (Figures 3 and 4). Characteristic spherical footprints of collapsed microcapsules with a random buckling pattern composed of folded regions were first observed at modest magnifications.

AFM images obtained at high resolution show fine grainy morphology with grain dimensions well below 50 nm, a common surface morphology of hydrogen-bonded LbL films. Surface topography of a swollen LbL shell assembled without PEI prime layer shows a relatively smooth surface morphology with the microroughness around 3 nm, which is noticeably higher than that measured for planar LbL films (Figure 5 and Table 1). We suggest that such increased microroughness value reflects additional film roughening caused by intense core release procedure. The overall thickness of these LbL shells with four bilayers is within 12–24 nm for different PVPON components which correspond to a single bilayer thickness of 3–6 nm, a common value for PVPON-based films in swollen state (Table 1).¹⁶

In contrast, the appearance of larger domains (around 100 nm) of segregated material has been observed for LbL shells in the presence

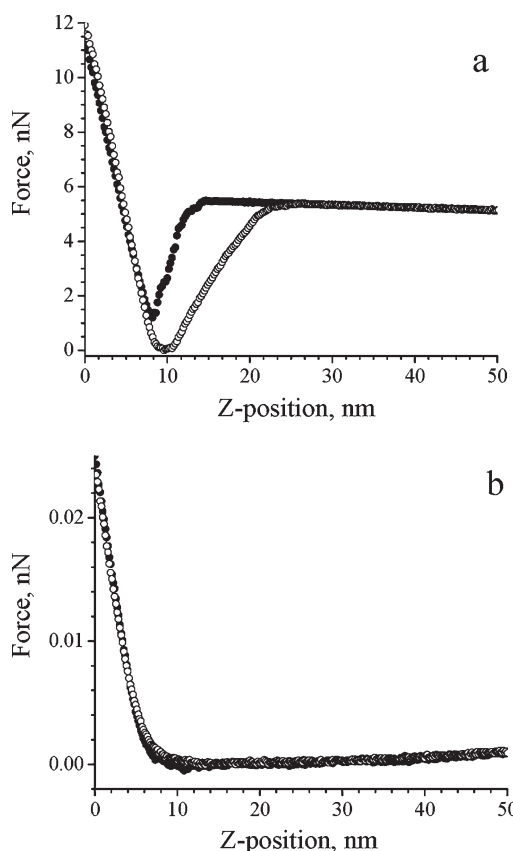


Figure 7. Force–distance curves for the dried (a) and swollen (b) PEI(TA/PVPON-1300) shell in air and water in an approaching–retracting cycle. Closed and open circles correspond to the approaching and retracting cycles, respectively.

of the PEI precursor. The formation of more developed domain morphology can be attributed to the stronger aggregation of polar tannic acid molecules in the presence of a positively charged PEI prime layer as has been discussed elsewhere.^{23,32} The microroughness also increases significantly from 4.9 ± 0.9 and 14.8 ± 2.3 nm due to localized swelling of the grainy shells (Table 1). These values are much higher than common values for polyelectrolyte LbL films (around 1 nm) and additionally confirm segregated nature of hydrogen-bonded LbL shells.⁷⁹

Mechanical Properties of LbL Shells. The histograms of surface distribution of the elastic modulus and adhesive forces as determined via the SFS technique over several selected surface areas of $1 \mu\text{m} \times 1 \mu\text{m}$ in both air and liquid environments are presented in Figure 6 (see details below). The average elastic modulus of the PEI(TA/PVPON-55) shell in water was determined from the corresponding histogram to be 0.89 ± 0.12 MPa with main contributions coming from flat surface areas. The apparent low-modulus fraction was caused by topographical contribution which originates from the local depletions in the shells.⁶⁶ The adhesion distribution is fairly wide as well due to highly variable contributions from uneven buckled, depleted, and flat surface areas of collapsed shells.

The representative examples of the force–distance curves employed for elastic modulus calculations obtained by averaging over multiple probing points are presented in Figure 7. In the dry state, a sharp snap-to contact point on the approaching curve and a clean snap-from pull-off point in the retracting curve are clearly

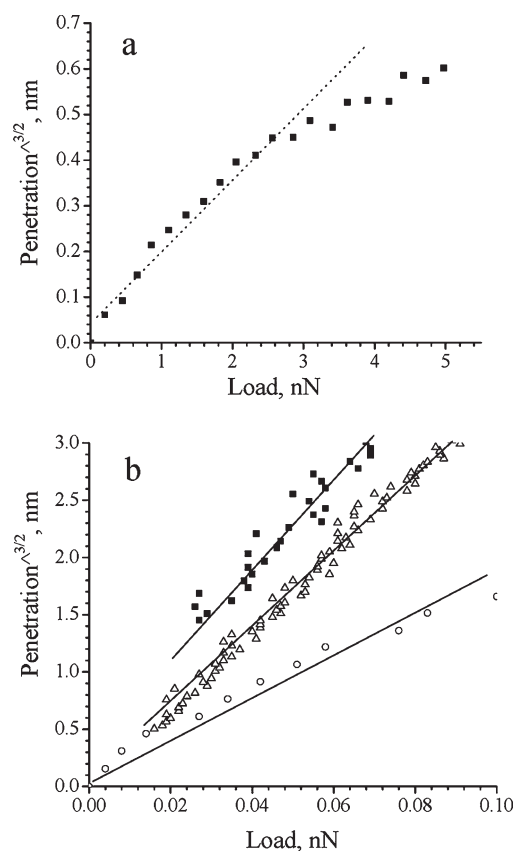


Figure 8. Experimental loading curves and fitting with Sneddon's model for the dry PEI(TA/PVPON-1300 kDa) (a) and swollen PEI(TA/PVPON) shells with different molecular weights (b): 1300 kDa (■), 360 kDa (△), and 55 kDa (○).

observed. High pull-off forces in the range of 6–10 nN are due to strong, capillary-driven interactions between hydrophilic AFM tip and modestly hydrophilic LbL surface.⁶⁵ Indeed, the contact angle of LbL films of 68° indicates the presence of the significant surface water layer at ambient conditions which facilitates liquid meniscus formation in tip–surface contact area.

After the placement the LbL shells in water the dramatic swelling was observed with 2–3-fold increase in the shell thickness (Table 1). The force–distance curves of the swollen capsule shells collected with much softer microcantilevers showed very little adhesion between the tip and the shell surface due to the elimination of the capillary forces (Figure 7). Indeed, the pull-off forces diminished by 2 orders of magnitude under these conditions. The slope of the force distance curves after physical contact also differs dramatically between dried and swollen shells, reflecting significant softening of the swollen shells after swelling by a factor of 3.

The deformational behavior of LbL shells can be quantified by converting force–distance data to loading curves which are represented in Hertzian coordinates in Figure 8. The loading curves derived for PEI(TA/PVPON-1300) shell in the dry state show that the linear behavior in Hertzian coordinates for almost entire range that indicates the elastic deformation (Figure 8).^{80,81} In addition, as could be seen from the loading curves the penetration depth is confined to about 10% of the film thickness (0.7 and 2 nm for dried and swollen, respectively) that precludes large influence of the silicon substrate. However, some deviation

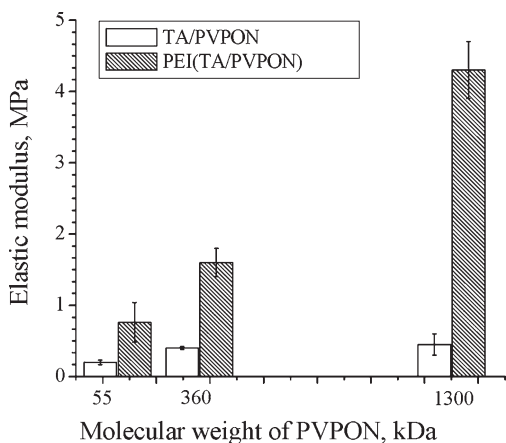


Figure 9. Young's modulus of swollen TA/PVPON shell vs molecular weight of PVPON with/without PEI prime layer.

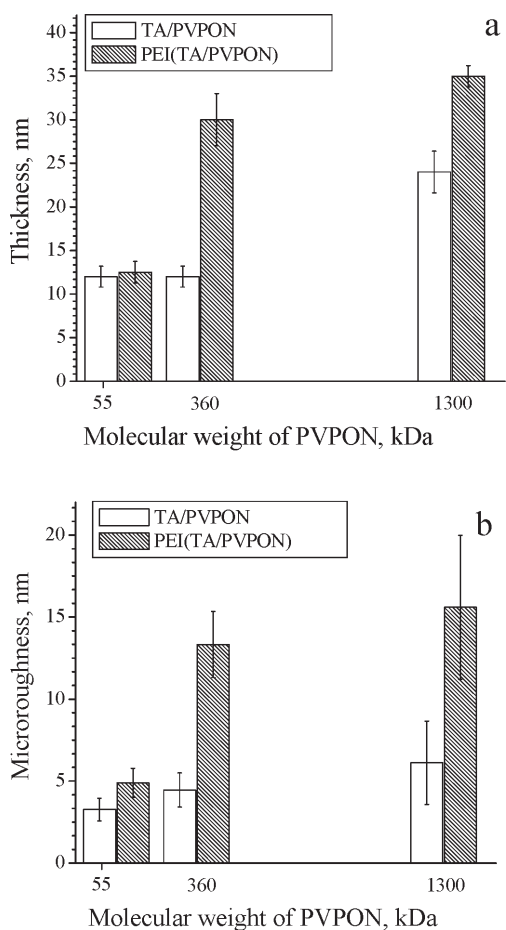


Figure 10. Thickness (a) and microroughness (b) of different types of LbL shells vs molecular weight of PVPON with and without PEI precursor.

from linear behavior at highest forces (above 3 nN for dry LbL film) is probably due to onset of plastic deformation. The elastic modulus was estimated from the applied loading data using the Sneddon's model was 600 ± 100 MPa, which is close to that measured for planar LbL films with similar composition (Table 1). Such similarities in elastic modulus values for planar

films and shells indicates that the process of assembling on silica cores followed by core release does not affect significantly the surface mechanical properties of LbL films even if surface morphology changes significantly.

All loading curves measured for swollen LbL shells with different molecular weights of PVPON show the same characteristics. The deformations reach about 2 nm under very light normal load below 100 pN (Figure 8). The linear character of the loading curves in Hertzian coordinates reflects purely elastic deformation under loading conditions exploited here.^{48,82} The slope of the loading curves varies significantly indicating a wide variation of the shell stiffness for different shell compositions. The estimated values of Young's modulus for LbL shells with different molecular weights of PVPON components and with/without PEI prime-layer derived from loading data are summarized in Figure 9 and Table 1.

As is apparent from this data, the elastic modulus values for the LbL shells vary in a wide range, more than an order of magnitude, from 0.2 ± 0.03 to 4.3 ± 0.4 MPa for different chemical compositions. First, LbL films without a PEI precursor layer are dramatically softened as compared with PEI-TA-PVPON shells (Figure 9). However, more than 2-fold stiffening is observed for the increasing molecular weight of PVPON component with the elastic modulus value increasing from to 0.45 MPa (Figure 9 and Table 1).

Similarly, the elastic modulus increased from 0.89 ± 0.12 to 4.3 ± 0.4 MPa as molecular weight of PVPON component increases for LbL films with PEI prime layer (Figure 9). Such a dramatic increase indicates the formation of an additional and dense network of physical entanglements due to more pronounced intermixing of the components and higher grafting density. Indeed, about 3-fold increase in the overall thickness is observed for swollen LbL films with high molecular weight PVPON component (Figure 10).

A significant stiffening of the LbL shells with increasing molecular weight of polymeric component observed here is in striking contrast to the common results for swollen polyelectrolyte LbL shells. In fact, for PAH/PSS shells, virtually unchanged elastic modulus was reported in the interval of molecular weights of different components from 15 000 to 1 000 000 Da.^{24,26} Such a stability of the deformational properties was explained by the fact that the local concentration of ionic cross-links is independent of molecular weight. We suggest that although this model might be applicable to polyanionic–polycationic LbL films with unaltered level of mixing of long chain components, for hydrogen-bonded LbL films studied here the level of intermixing of low molar weight and long chain components changes significantly for increasing molecular weight of PVPON (Table 1 and Figure 10).

Second, it is worth to note that the measured elastic modulus of the swollen TA/PVPON shells both with PEI precursor (0.89 – 4.3 MPa) and without PEI (0.2 – 0.45 MPa) falls within the range of expected moduli for gel materials which have modest-to-high cross-linking densities which is consistent with high concentration of binding sites of TA component.⁸³ Indeed, comparative values of elastic modulus from 0.06 to 0.8 MPa were reported by Boudou et al.⁸⁴ for electrostatically bonded polyelectrolyte multilayer films with natural components such as poly(L-lysine)/hyaluronan, chitosan/hyaluronan, and PAH/poly(L-glutamic acid) as measured by the AFM nanoindentation method. However, a significantly higher elastic modulus of 600 MPa was obtained by Elsner et al. for swollen hydrogen-bonded

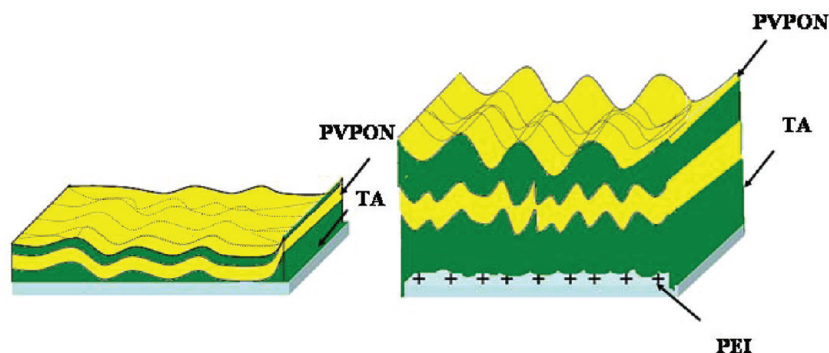


Figure 11. Schematics of TA/PVPON shell morphologies without and with PEI prelayer.

PMAA/PVPON multilayer in buffer.² The range of values of 100–200 MPa for various LbL shells was reported by Vinogradova et al.,⁸⁵ who determined elastic properties using both AFM deformation and osmotic swelling. The much higher values of 1.5–2 GPa were measured by Dubreuil and co-workers PSS/PAH microcapsules by osmotic-driven collapse and reflection interference contrast microscopy.⁵¹

The reasons for such divergence in the Young's modulus values for different LbL multilayers are commonly attributed to significant differences in the intermolecular interactions involved and the intermixing behavior. For instance, by the variation of the initial parameters of synthesis, such as solvent for core release and buffer parameters the elastic properties of swollen PAH/PSS shell can be reduced from 100 to 30 MPa.^{24,34,86} The significant reduction of elastic modulus down to 10 MPa at high pH was explained by a reduction of component interactions, packing density of components, and even pore formation. The reduction of the Young's modulus of PAH/PSS capsules with improved degree of stretching caused by thermal post-treatment has been considered by Kim et al.⁸⁷ The effect of organic solvent on the polyelectrolyte/phosphorus dendrimer multilayer stiffening due to the screening of the electrostatic interaction between polyelectrolytes was reported.⁸⁸ According to Boudou et al., a significant effect of stiffening on multilayer shells could also be reached at certain concentration of cross-linking sites.⁸⁴ For example, for chitosan/hyaluronan multilayer films, the Young's modulus increased from 63 to 187 kPa when the concentration of cross-linker increased 10-fold. The elastic modulus of chitosan/hyaluronan LbL shells at a high concentration of cross-linking (100 mg/mL) was measured to be 3 times higher than the native LbL film while the elastic modulus of the poly(L-lysine)/hyaluronan film is 2 times higher at same concentration of cross-linking agent.⁸⁴

Accordingly, the variation of the elastic modulus observed in this study can be related to the variation of corresponding morphological characteristics which are summarized in Figure 11. This general trend in an alternation of mechanical properties is common for all LbL films studied here. However, significant differences are caused by presence/absence of PEI prime layer. We can suggest that the deposition of PEI prime layers reverses the surface charge of naturally negatively charged silica cores, which leads to the enhanced adsorption of polar TA molecules on positively charged PEI surface and thus an increased probability for multiple binding of PVPON component and thus increased thickness of the LbL shells. Moreover, the ionization of weak polyacid within the polyelectrolyte multilayers reinforces the hydrogen-bonding interaction between TA and PVPON

components that significantly effects the aggregation and intermixing status within LbL shells. Indeed, all LbL shells with cationic PEI layer show much higher thicknesses (30–50% higher) as compared to LbL shells without a PEI component (Table 1). A higher level of intermixing and aggregation of components in the presence of the PEI is supported by significantly increased microroughness of LbL films with PEI prime layer.

CONCLUSION

In conclusion, we reported on the mechanical properties and surface morphology of hydrogen-bonded TA/PVPON LbL shells. In a dry state, the value of the elastic modulus was measured about 1 GPa for both planar film and LbL shell with the same composition. Such an agreement indicates that LbL assembly on a microparticles followed by their dissolution does not affect significantly the physical properties of LbL multilayers. This value is in agreement with but lower than the elastic modulus value for electrostatically assembled LbL films due to the presence of residual water and weak hydrogen bonding.

In contrast, swelling of LbL shells up to 3-fold results in dramatic reduction of the elastic modulus down to 0.2–0.4 MPa, a common value for highly compliant densely cross-linked gel materials. The values measured for TA/PVPON is much lower than that for traditional LbL shells in the swollen state (hundreds MPa). The increase of the molecular weight of the PVPON component from 55 to 1300 kDa promotes chain entanglements and intermixing that causing significant stiffening of LbL shells with the elastic modulus rising from 0.2 to 0.45 MPa for PEI-free LbL shells. Moreover, adding a PEI prime layer to the core before LbL shell assembly dramatically affects the growth and aggregation state of hydrogen-bonded multilayers which consequently results in dramatically stiffer, thicker, and rougher shells with the elastic modulus reaching 4.3 MPa for high molecular PVPON component.

Such a fine-tuning of the elastic properties of very compliant hydrogen-bonded shells with elastic modulus from 0.2 to 4.3 MPa with fine-tuning in their chemical composition is a characteristic feature of weakly bonded LbL shells in contrast to traditional polyelectrolyte LbL assemblies. Assembling a cationic primary layer and variation of molecular weight of polymer layers allows to control thickness and stiffness of the capsule shell which is crucial for the potential applications in drug release and sensor platforms. The ability to tune the elastic modulus is critically important for the design of compliant LbL shells with controlled

mechanical stability, loading/unloading capabilities, and permeability.

AUTHOR INFORMATION

Corresponding Author

*E-mail: vladimir@mse.gatech.edu.

ACKNOWLEDGMENT

This work was supported by the Air Force Office of Scientific Research FA9550-08-1-0446, FA9550-09-1-0162 grants, and the DoD through the NDSEG program for K.D.A. The authors acknowledge V. Kozlovskaya for technical assistance.

REFERENCES

- (1) Volodkin, D.; Skirtach, A.; Mohwald, H. *Adv. Polym. Sci.* **2011**, 239, 1.
- (2) Elsner, N.; Kozlovskaya, V.; Sukhishvili, S. A.; Fery, A. *Soft Matter* **2006**, 2, 966.
- (3) Quinn, J. F.; Johnston, A. P. R.; Such, G. K.; Zelikin, A. N.; Caruso, F. *Chem. Soc. Rev.* **2007**, 36, 707.
- (4) Wilson, J. T.; Chaikof, E. L. *Adv. Drug Delivery Rev.* **2008**, 60, 124.
- (5) Ariga, K.; Ji, Q.; Hill, J. P. *Adv. Polym. Sci.* **2010**, 229, 51.
- (6) Shutava, T. G.; Balkundi, S. S.; Vangala, P.; Steffan, J. J.; Bigelow, R. L.; Cardelli, J. A.; O'Neal, D. P.; Lvov, Y. M. *ACS Nano* **2009**, 3, 1877.
- (7) Sukhorukov, G.; Möhwald, H. *Trends Biotechnol.* **2007**, 25, 93.
- (8) Volodkin, D. V.; Petrov, A. I.; Prevot, M.; Sukhorukov, G. B. *Langmuir* **2004**, 20, 3398.
- (9) Ai, H.; Fang, M.; Jones, S.; Lvov, Y. *Biomacromolecules* **2002**, 3, 560.
- (10) Khutoryanskiy, V. *Int. J. Pharm.* **2007**, 334, 15.
- (11) Kharlampieva, E.; Sukhishvili, S. A. *J. Macromol. Sci., Polym. Rev.* **2006**, 46, 377.
- (12) Lavalle, P.; Voegel, J. C.; Vautier, D.; Senger, B.; Schaaf, P.; Ball, V. *Adv. Mater.* **2011**, 23, 1191.
- (13) Quinn, J. E.; Caruso, F. *Aust. J. Chem.* **2005**, 58, 442.
- (14) Kozlovskaya, V.; Kharlampieva, E.; Khanal, B. P.; Manna, P.; Zubarev, E. R.; Tsukruk, V. V. *Chem. Mater.* **2008**, 20, 7474.
- (15) Sukhishvili, S. A.; Granick, S. *Macromolecules* **2002**, 35, 301.
- (16) Kozlovskaya, V.; Harbaugh, S.; Drachuk, I.; Shchepelina, O.; Kelley-Loughnane, N.; Stone, M.; Tsukruk, V. V. *Soft Matter* **2011**, 7, 2364.
- (17) Wilson, J. T.; Cui, W.; Kozlovskaya, V.; Kharlampieva, E.; Pan, D.; Qu, Z.; Krishnamurthy, V. R.; Mets, J.; Kumar, V.; Wen, J.; Song, Y.; Tsukruk, V. V.; Chaikof, E. L. *J. Am. Chem. Soc.* **2011**, 133, 7054.
- (18) Zhang, W.; Zhang, A.; Guan, Y.; Zhang, Y.; Zhu, X. X. *J. Mater. Chem.* **2011**, 21, 548.
- (19) Lee, D.; Cohen, R. E.; Rubner, M. F. *Langmuir* **2005**, 21, 9651.
- (20) Erel-Unal, I.; Sukhishvili, S. A. *Macromolecules* **2008**, 41, 3962.
- (21) Desiraju, G. R. In *Encyclopedia of Supramolecular Chemistry*; Marcel Dekker: New York, 2004.
- (22) Shutava, T.; Prouty, M.; Kommireddy, D.; Lvov, Y. *Macromolecules* **2005**, 38, 2850.
- (23) Carter, J. L.; Drachuk, I.; Harbaugh, S.; Kelley-Loughnane, N.; Stone, M.; Tsukruk, V. V. *Macromol. Biosci.* **2011**.
- (24) Fery, A.; Weinkamer, R. *Polymer* **2007**, 48, 7221.
- (25) Vinogradova, O.; Lebedeva, O. V.; Kim, B. S. *Annu. Rev. Mater. Res.* **2006**, 36, 143.
- (26) Lulevich, V. V.; Nordschild, S.; Vinogradova, O. I. *Macromolecules* **2004**, 37, 7736.
- (27) Antipov, A. A.; Sukhorukov, G. B.; Möhwald, H. *Langmuir* **2003**, 19, 2444.
- (28) Sukhorukov, G. B.; Fery, A.; Brumen, M.; Möhwald, H. *Phys. Chem. Chem. Phys.* **2004**, 6, 4078.
- (29) Fernandes, P. A. L.; Delcea, M.; Skirtach, A. G.; Möhwald, H.; Fery, A. *Soft Matter* **2010**, 6, 1879.
- (30) Esser-Kahn, A. P.; Sottos, N. R.; White, S. R.; Moore, J. S. *J. Am. Chem. Soc.* **2010**, 132, 10266.
- (31) Gao, C.; Leporatti, S.; Moya, S.; Donath, E.; Möhwald, H. *Langmuir* **2001**, 17, 3491.
- (32) Kozlovskaya, V.; Kharlampieva, E.; Drachuk, I.; Cheng, D.; Tsukruk, V. V. *Soft Matter* **2010**, 6, 3596.
- (33) Skirtach, A. G.; Dejumat, C.; Braun, D.; Sussha, A. S.; Rogach, A. L.; Parak, W. J.; Möhwald, H.; Sukhorukov, G. B. *Nano Lett.* **2005**, 5, 1371.
- (34) Lulevich, V. V.; Vinogradova, O. I. *Langmuir* **2004**, 20, 2874.
- (35) Guan, Y.; Zhang, Y.; Zhou, T.; Zhou, S. *Soft Matter* **2009**, 5, 842.
- (36) Nolte, A. J.; Cohen, R. E.; Rubner, M. F. *Macromolecules* **2006**, 39, 4841.
- (37) Singamaneni, S.; Tsukruk, V. V. *Soft Matter* **2010**, 6, 5681.
- (38) Nolte, A. J.; Rubner, M. F.; Cohen, R. E. *Macromolecules* **2005**, 38, 5367.
- (39) Stafford, C. M.; Harrison, C.; Beers, K. L.; Karim, A.; Amis, E. J.; VanLandingham, M. R.; Kim, H. C.; Volksen, W.; Miller, R. D.; Simonyi, E. E. *Nature Mater.* **2004**, 3, 545.
- (40) Jiang, C.; Singamaneni, S.; Merrick, E.; Tsukruk, V. V. *Nano Lett.* **2006**, 6, 2254.
- (41) Markutsya, S.; Jiang, C.; Pikus, Y.; Tsukruk, V. V. *Adv. Funct. Mater.* **2005**, 15, 771.
- (42) Jiang, C.; Markutsya, S.; Pikus, Y.; Tsukruk, V. V. *Nature Mater.* **2004**, 3, 721.
- (43) Jiang, C.; Kommireddy, D. S.; Tsukruk, V. V. *Adv. Funct. Mater.* **2006**, 16, 27.
- (44) Gunawidjaja, R.; Jiang, C.; Ko, H.; Tsukruk, V. V. *Adv. Mater.* **2006**, 18, 2895.
- (45) Jiang, C.; Markutsya, S.; Shulha, H.; Tsukruk, V. V. *Adv. Mater.* **2005**, 17, 1669.
- (46) Jiang, C.; Ko, H.; Tsukruk, V. V. *Adv. Mater.* **2005**, 17, 2127.
- (47) Ko, H.; Jiang, C.; Shulha, H.; Tsukruk, V. V. *Chem. Mater.* **2005**, 17, 2490.
- (48) Lebedeva, O. V.; Kim, B. S.; Vasilev, K.; Vinogradova, O. I. *J. Colloid Interface Sci.* **2005**, 284, 455.
- (49) Gao, C.; Donath, E.; Moya, S.; Dudnik, V.; Mohwald, H. *Eur. Phys. J. E* **2001**, 5, 21.
- (50) Sukhorukov, G. B.; Fery, A.; Brumen, M.; Mohwald, H. *Phys. Chem. Chem. Phys.* **2004**, 6, 4078.
- (51) Dubreuil, F.; Elsner, N.; Fery, A. *Eur. Phys. J. E* **2003**, 12, 215.
- (52) Delcea, M.; Schmidt, S.; Palankar, R.; Fernandes, P. A. L.; Fery, A.; Möhwald, H.; Skirtach, A. G. *Small* **2010**, 6, 2858.
- (53) Fery, A.; Dubreuil, F.; Möhwald, H. *New J. Phys.* **2004**, 6, 18.
- (54) Lu, C.; Donch, I.; Nolte, M.; Fery, A. *Chem. Mater.* **2006**, 18, 6204.
- (55) Heuvingh, J.; Zappa, M.; Fery, A. *Langmuir* **2005**, 21, 3165.
- (56) Lulevich, V. V.; Radtchenko, I. L.; Sukhorukov, G. B.; Vinogradova, O. I. *Macromolecules* **2003**, 36, 2832.
- (57) Peleshanko, S.; Julian, M. D.; Ornatska, M.; McConney, M. E.; LeMieux, M. C.; Chen, N.; Tucker, C.; Yang, Y.; Liu, C.; Humphrey, J. A. C.; Tsukruk, V. V. *Adv. Mater.* **2007**, 19, 2903.
- (58) Lemieux, M.; Minko, S.; Usov, D.; Stamm, M.; Tsukruk, V. V. *Langmuir* **2003**, 19, 6126.
- (59) Julthongpiput, D.; LeMieux, M.; Tsukruk, V. V. *Polymer* **2003**, 44, 4557.
- (60) Tsukruk, V. V.; Sidorenko, A.; Gorbunov, V. V.; Chizhik, S. A. *Langmuir* **2001**, 17, 6715.
- (61) McConney, M. E.; Singamaneni, S.; Tsukruk, V. V. *Polym. Rev.* **2010**, 50, 235.
- (62) Müller, R.; Köhler, K.; Weinkamer, R.; Sukhorukov, G. B.; Fery, A. *Macromolecules* **2005**, 38, 9766.
- (63) Kovalev, A.; Shulha, H.; Lemieux, M.; Myshkin, N.; Tsukruk, V. V. *J. Mater. Res.* **2004**, 19, 716.
- (64) Shulha, H.; Kovalev, A.; Myshkin, N.; Tsukruk, V. V. *Eur. Polym. J.* **2004**, 40, 949.

- (65) Tsukruk, V. V.; Bliznyuk, V. N. *Langmuir* **1998**, *14*, 446.
- (66) Lemieux, M.; Usov, D.; Minko, S.; Stamm, M.; Shulha, H.; Tsukruk, V. V. *Macromolecules* **2003**, *36*, 7244.
- (67) Podsiadlo, P.; Arruda, E. M.; Kheng, E.; Waas, A. M.; Lee, J.; Critchley, K.; Qin, M.; Chuang, E.; Kaushik, A. K.; Kim, H. S.; Qi, Y.; Noh, S. T.; Kotov, N. A. *ACS Nano* **2009**, *3*, 1564.
- (68) Jiang, C.; Wang, X.; Gunawidjaja, R.; Lin, Y.-H.; Gupta, M. K.; Kaplan, D. L.; Naik, R. R.; Tsukruk, V. V. *Adv. Funct. Mater.* **2007**, *17*, 2229.
- (69) Bartkowiak, A.; Hunkeler, D. *Chem. Mater.* **1999**, *11*, 2486.
- (70) Jiang, C.; Tsukruk, V. V. *Adv. Mater.* **2006**, *18*, 829.
- (71) Kharlampieva, E.; Kozlovskaya, V.; Gunawidjaja, R.; Shevchenko, V. V.; Vaia, R.; Naik, R. R.; Kaplan, D. L.; Tsukruk, V. V. *Adv. Funct. Mater.* **2010**, *20*, 840.
- (72) Lavalle, P.; Voegel, J.-C.; Vautier, D.; Senger, B.; Schaaf, P.; Ball, V. *Adv. Mater.* **2011**, *23*, 1191.
- (73) Kozlovskaya, V.; Kharlampieva, E.; Jones, K.; Lin, Z.; Tsukruk, V. V. *Langmuir* **2010**, *26*, 7138.
- (74) Tsukruk, V. V.; Reneker, D. H. *Polymer* **1995**, *36*, 1791.
- (75) Sidorenko, A.; Ahn, H.; Kim, D.; Yang, H.; Tsukruk, V. V. *Wear* **2002**, *252*, 946.
- (76) Tsukruk, V. V.; Huang, Z.; Chizhik, S. A.; Gorbunov, V. V. *J. Mater. Sci.* **1998**, *33*, 4905.
- (77) Tsukruk, V. V.; Gorbunov, V. V. *Probe Microsc.* **2002**, *3*, 241.
- (78) Choi, I.; Suntivich, R.; Plamper, F. A.; Synatschke, C. V.; Mueller, A. H. E.; Tsukruk, V. V. *J. Am. Chem. Soc.* **2011**, *133*, 9592.
- (79) Lin, Y. H.; Teng, J.; Zubarev, E. R.; Shulha, H.; Tsukruk, V. V. *Nano Lett.* **2005**, *5*, 491.
- (80) Chizhik, S. A.; Huang, Z.; Gorbunov, V. V.; Myshkin, N. K.; Tsukruk, V. V. *Langmuir* **1998**, *14*, 2606.
- (81) Domke, R.; Radmacher, M. *Langmuir* **1998**, *14*, 3320.
- (82) Pharr, G. M.; Oliver, W. C.; Brotzen, F. B. *J. Mater. Res.* **1992**, *7*, 613.
- (83) Sperling, L. H. *Polymeric Multicomponent Materials*; Wiley-VCH: New York, 1997.
- (84) Boudou, T.; Crouzier, T.; Auzely-Velty, R.; Glinel, K.; Picart, C. *Langmuir* **2009**, *25*, 13809.
- (85) Vinogradova, O. I.; Andrienko, D.; Lulevich, V. V.; Nordschild, S.; Sukhorukov, G. B. *Macromolecules* **2004**, *37*, 1113.
- (86) Gao, C.; Leporatti, S.; Moya, S.; Donath, E.; Möhwald, H. *Chem.—Eur. J.* **2003**, *9*, 915.
- (87) Kim, B. S.; Fan, T. H.; Vinogradova, O. *Soft Matter* **2011**, *7*, 2705.
- (88) Kim, B. S.; Lebedeva, O. V.; Park, M. K.; Knoll, W.; Caminade, A. M.; Majoral, J. P.; Vinogradova, O. I. *Polymer* **2010**, *51*, 4525.